Proceedings of the 13th
KACC, October 1998

Investigation of the Different Control Approaches for a Remote Sensing Satellite Attitude Control

Chang-Hee Won and Jeong-Sook Lee

Satellite Communications System Department,
Electronics and Telecommunications Research Institute,
Yusong P.O. Box 106, Taejon, Korea 305-600
Tel: (82-42) 860-4876, Fax: (82-42) 860-6949, Email: won@etri.re.kr

Abstract

A nonlinear attitude model of a satellite with thrusters, magnetic torquers and a reaction wheel cluster is developed. Then the linearized version of this satellite attitude model is derived for the attitude hold mode. For comparison purpose, various control methods are considered for attitude control of a satellite. We consider a proportional derivative controller which is actually used in the remote sensing satellite, KOMPSAT. Then a comparison is made with an H_2 controller, an H_∞ controller, and a mixed H_2/H_∞ controller. The analysis and numerical studies show that the proportional derivative controller's performance is limited in the sense that the pitch angle cannot approach zero. The simulations also show that among three control methods (H_2 control, H_∞ control, and mixed H_2/H_∞ control) H_2 control has the fastest response time, H_∞ control has the slowest and mixed H_2/H_∞ control comes in between the first two control methods. On the other hand, H_∞ control used least amount of control effort while H_2 control required the most.

1. Introduction

The desire and need to precisely control a spacecraft's attitude lead to active research in the satellite attitude control area throughout the years. In the paper by Wie and *et al.*, a new approach to control the attitude of the space station has been proposed [5]. There they found the linearized equation of motion and attitude kinematics and used the LQR and pole placement techniques to control the attitude of the space station. In 1996, Ballois and Duc noted that a new LQR controller has been synthesized for one position of the solar array, and the controller change is needed for other positions. Thus they proposed an H_∞ controller to meet the performance and robustness objectives [1]. As recently as 1997, Kida *et al.* have compared linear quadratic Gaussian control with H_∞ control for a flexible spacecraft ETS-VI [3]. Even though various control methods have been used throughout the literature, to the best of our knowledge, a comparison of the spacecraft attitude control methods using PD, H_2 control, H_∞ control, and mixed H_2/H_∞ control have not been done. The application of mixed H_2/H_∞ control to spacecraft attitude control also has not been done in the literature.

2. Nonlinear Satellite Attitude Model

We begin the discussion by defining the local vertical local horizontal (LVLH) coordinate system. The z-axis of the LVLH coordinate system originates at the center of mass of the satellite and passes through the center of the earth. The y-axis points in the opposite direction of instantaneous orbital angular momentum vector. The direction of the x-axis is chosen to complete the right-handed coordinate system and is in the direction of the spacecraft velocity. This LVLH system does not rotate with the body of the spacecraft. The origin of body fixed coordinate (BFC) is fixed at the satellite mass center and rotates with the satellite at angular rate, ω. The z-axis of the BFC is defined as the axis of symmetry of the spacecraft primary axis, the x-axis is perpendicular to the z-axis and passes through a fixed point on the spacecraft body, and the y-axis completes the right handed triad. Consider a satellite with four thrusters, three magnetic torquers, and a four reaction wheel cluster as the actuators. Then the general nonlinear satellite attitude dynamics model can be described as

$$I_g \dot{\underline{\omega}} = -\underline{\omega} \times (I_t \underline{\omega} + L' I_w \underline{\Omega}) - L' \underline{\tau}_w + \underline{\tau}_{thruster} + \underline{\tau}_{gravity} + \underline{\tau}_{aero} + \underline{\tau}_{magnetic} + \underline{\tau}_{srp} \quad (1)$$

$$\dot{\underline{h}}_w = \underline{\tau}_w \quad (2)$$

$$\underline{h}_w = I_w \underline{\Omega} + I_w L \underline{\omega} \quad (3)$$

where I_t : Total moment of inertia for the satellite body (3x3), I_w : Moment of inertial matrix for the wheels (4x4), $I_g = I_t - L' I_w L$: Total moment of inertia minus the moment of inertia of the wheels (3x3), L : Wheel orientation matrix (4x3), $\underline{\omega}$: Angular velocity vector in BFC (3x1), $\underline{\Omega}$: Wheel speed vector, $\underline{\tau}_w$: Absolute torque due to the reaction wheels, $\underline{\tau}_{thruster}$: Torque due to the thrusters, $\underline{\tau}_{gravity}$: Torque due to the Earth's gravity gradient, $\underline{\tau}_{aero}$: Aerodynamic torque due to the atmospheric drag, $\underline{\tau}_{magnetic}$: Torque due to the magnetic field, $\underline{\tau}_{srp}$: Torque due to the solar radiation pressure, $\underline{h}_w$: Angular momentum of the wheel cluster, and the prime, ('), notation is used to denote

the transposition. Figure 1 shows the configuration of four reaction wheels. The orientation matrix L is given by

$$L = \begin{bmatrix} \cos\alpha\sin\beta & \sin\alpha\sin\beta & \cos\beta \\ -\sin\alpha\sin\beta & \cos\alpha\sin\beta & \cos\beta \\ -\cos\alpha\sin\beta & -\sin\alpha\sin\beta & \cos\beta \\ \sin\alpha\sin\beta & -\cos\alpha\sin\beta & \cos\beta \end{bmatrix}. \quad (4)$$

From Equations (1), (2), and (3), we obtain the wheel dynamics equation. Take time derivative of Equation (3) and substitute it into Equation (2). Then solve for the $\dot{\underline{\Omega}}$. This gives the wheel dynamics equation:

$$\dot{\underline{\Omega}} = I_w^{-1}\underline{\tau}_w - L\dot{\underline{\omega}} \quad (5)$$

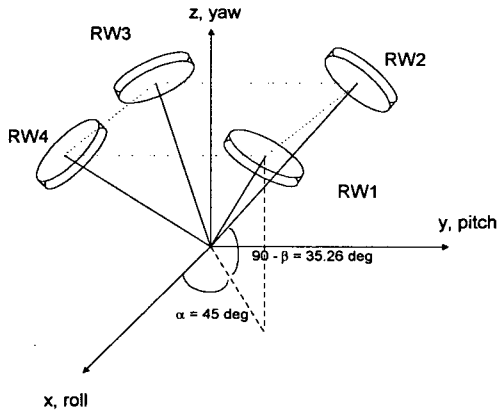

Figure 1: Reaction wheel cluster configuration in BFC

Now, substitute Equation (1) into Equation (5) to obtain,

$$\dot{\underline{\Omega}} = I_w^{-1}\underline{\tau}_w - L[-I_g^{-1}\underline{\omega}\times(I_t\underline{\omega} + L'I_w\Omega) + I_g^{-1}(\underline{\tau}_{thruster} + \underline{\tau}_{gravity} + \underline{\tau}_{aero} + \underline{\tau}_{magnetc} + \underline{\tau}_{srp} - L'\underline{\tau}_w)] \quad (6)$$

Attitude control requires coordinate transformation from LVLH to BFC. To keep the satellite attitude Earth pointing, the satellite body axes have to be aligned with LVLH axes. Pitch (θ)-yaw (ψ)-roll (ϕ) transformation matrix can be represented using Euler angles as follows.

$$\begin{bmatrix} x \\ y \\ z \end{bmatrix}_{BFC} = \begin{bmatrix} \cos\psi\cos\theta & \sin\psi & -\cos\psi\sin\theta \\ -\cos\phi\sin\psi\cos\theta + \sin\phi\sin\theta & \cos\phi\cos\psi & \cos\phi\sin\psi\sin\theta + \sin\phi\cos\theta \\ \sin\phi\sin\psi\cos\theta + \cos\phi\sin\theta & -\sin\phi\cos\psi & -\sin\phi\sin\psi\sin\theta + \cos\phi\cos\theta \end{bmatrix} \begin{bmatrix} x_L \\ y_L \\ z_L \end{bmatrix}_{LVLH}$$

$$\equiv [\underline{c}_1 \;\; \underline{c}_2 \;\; \underline{c}_3] \begin{bmatrix} x_L \\ y_L \\ z_L \end{bmatrix}_{LVLH} \quad (7)$$

On the other hand, Pitch-yaw-roll body-axes sequence attitude kinematics are represented by

$$\begin{bmatrix} \dot{\phi} \\ \dot{\theta} \\ \dot{\psi} \end{bmatrix} = \frac{1}{\cos\psi}\begin{bmatrix} \cos\psi & -\cos\phi\sin\psi & \sin\phi\sin\psi \\ 0 & \cos\phi & -\sin\phi \\ 0 & \sin\phi\cos\psi & \cos\phi\cos\psi \end{bmatrix}\begin{bmatrix} \omega_x \\ \omega_y \\ \omega_z \end{bmatrix} + \begin{bmatrix} 0 \\ n \\ 0 \end{bmatrix},$$

where n is the orbital rate. (8)

3. Linear Satellite Attitude Model

Here we consider controlling the satellite's attitude using a cluster of reaction wheels and thrusters. For the LEO satellites with the altitude from 400km to 2500km, the largest torque is the gravitational torque. See [2, p.271]. Thus we incorporate the gravitational torque into the system equation. The second and third largest torques affecting the satellites are the aerodynamic torque and the magnetic torque. Thus we consider these torques as the external disturbances. The solar radiation pressure (diffuse reflection and specular reflections), the effects due to luni solar gravitation, and charged particles are ignored because they are much smaller than the gravitational, magnetic and aerodynamic torques [2, p.271]. The gravity gradient torque for a point mass is given by [3, p.286]

$$\underline{\tau}_{gravity} = 3n^2\underline{c}_3^{\times}I_t\underline{c}_3 \quad (9)$$

where n is the orbital angular rate, and $\underline{c}_3^{\times}$ represents the cross product matrix of a vector $\underline{c}_3$ defined in Equation (7).

Thus Equation (1) becomes

$$I_g\dot{\underline{\omega}} = -\underline{\omega}\times(I_t\underline{\omega} + L'I_w\underline{\Omega}) - L'\underline{\tau}_w + \underline{\tau}_{thruster} + 3n^2\underline{c}_3^{\times}I_t\underline{c}_3 + \underline{w} \quad (10)$$

where $\underline{w} = \underline{\tau}_{aero} + \underline{\tau}_{magnetc} + \underline{\tau}_{srp}$.

If we assume small attitude variations from LVLH coordinate, the above equation can be linearized in the state space form around a certain equilibrium point as follows:

$$\dot{\underline{x}} = \left(\frac{\partial f}{\partial \underline{x}'}\right)\underline{x} + \left(\frac{\partial f}{\partial \underline{u}'}\right)\underline{u} + \left(\frac{\partial f}{\partial \underline{w}'}\right)\underline{w} \quad (11)$$

$$\dot{\underline{x}} = A\underline{x} + B\underline{u} + E\underline{w} \quad (12)$$

where

$\underline{x} = [\phi,\theta,\psi,\omega_x,\delta\omega_y,\omega_z,\Omega_1,\Omega_2,\Omega_3,\Omega_4]' \equiv [\underline{\phi}_e,\underline{\omega},\underline{\Omega}]'$ and $\underline{u} = [\underline{\tau}_w \;\; \underline{\tau}_{thruster}]'$.

To have zero initial conditions we let $\delta\omega_y = \omega_y + n$, and find the general linear equation for any torque equilibrium attitude (TEA) of the states. For the simplicity sake, here we assume the case of the attitude hold mode where the TEA values are fixed at the following values:

$\underline{x}_0 = [0,0,0,0,0,0,0,0,0,0]'$. Then the following matrices can be defined

$$I_t = \begin{bmatrix} It(1,1) & It(1,2) & It(1,3) \\ It(2,1) & It(2,2) & It(2,3) \\ It(3,1) & It(3,2) & It(3,3) \end{bmatrix}$$

$$Iw = diag[Iw(1,1), Iw(2,2), Iw(3,3), Iw(4,4)]$$

$$L' = \begin{bmatrix} Lt(1,1) & Lt(1,2) & Lt(1,3) & Lt(1,4) \\ Lt(2,1) & Lt(2,2) & Lt(2,3) & Lt(2,4) \\ Lt(3,1) & Lt(3,2) & Lt(3,3) & Lt(3,4) \end{bmatrix}$$

$$I_g^{-1} = \begin{bmatrix} Iginv(1,1) & Iginv(1,2) & Iginv(1,3) \\ Iginv(2,1) & Iginv(2,2) & Iginv(2,3) \\ Iginv(3,1) & Iginv(3,2) & Iginv(3,3) \end{bmatrix}$$

$$\underline{\tau}_w' = [\tau_{w1} \quad \tau_{w2} \quad \tau_{w3} \quad \tau_{w4}]. \tag{13}$$

Now we expand the right hand side of Equation (10), and then linearize around the TEA, we obtain the following linear equations from Equation (10).

$$I_g \dot{\underline{\omega}} = n \begin{bmatrix} It(3,1) & 2It(3,2) & It(3,3)-It(2,2) \\ -It(3,2) & 0 & It(1,2) \\ It(2,2)-It(1,1) & -2It(1,2) & -It(1,3) \end{bmatrix} \begin{bmatrix} \omega_x \\ \delta\omega_y \\ \omega_z \end{bmatrix}$$
$$+ n \begin{bmatrix} Iw(1,1)Lt(3,1) & Iw(2,2)Lt(3,2) & Iw(3,3)Lt(3,3) & Iw(4,4)Lt(3,4) \\ 0 & 0 & 0 & 0 \\ -Iw(1,1)Lt(1,1) & -Iw(2,2)Lt(1,2) & -Iw(3,3)Lt(1,3) & -Iw(4,4)Lt(1,4) \end{bmatrix} \begin{bmatrix} \Omega_1 \\ \Omega_2 \\ \Omega_3 \\ \Omega_4 \end{bmatrix}$$
$$+ 3n^2 \begin{bmatrix} It(3,3)-It(2,2) & It(2,1) & 0 \\ It(2,1) & It(3,3)-It(1,1) & 0 \\ -It(1,3) & -It(2,3) & 0 \end{bmatrix} \begin{bmatrix} \phi \\ \theta \\ \psi \end{bmatrix} + n^2 \begin{bmatrix} -2It(2,3) \\ 3It(1,3) \\ -It(1,2) \end{bmatrix} - L' \underline{\tau}_w + \underline{\tau}_{thruster} + \underline{w} \tag{14}$$

Assuming that the products of inertia of the satellite body are small, we obtain

$$\dot{\underline{\omega}} \equiv I_g^{-1} nN_1 \begin{bmatrix} \omega_x \\ \delta\omega_y \\ \omega_z \end{bmatrix} + I_g^{-1} nN_2 \begin{bmatrix} \Omega_1 \\ \Omega_2 \\ \Omega_3 \\ \Omega_4 \end{bmatrix} + I_g^{-1} 3n^2 N_3 \begin{bmatrix} \phi \\ \theta \\ \psi \end{bmatrix} \tag{15}$$
$$- I_g^{-1} L' \underline{\tau}_w + I_g^{-1} \underline{\tau}_{thruster} + I_g^{-1} \underline{w}$$

where

$$N_1 = \begin{bmatrix} 0 & 0 & It(3,3)-It(2,2) \\ 0 & 0 & 0 \\ It(2,2)-It(1,1) & 0 & 0 \end{bmatrix}$$

$$N_2' = \begin{bmatrix} Iw(1,1)Lt(3,1) & 0 & -Iw(1,1)Lt(1,1) \\ Iw(2,2)Lt(3,2) & 0 & -Iw(2,2)Lt(1,2) \\ Iw(3,3)Lt(3,3) & 0 & -Iw(3,3)Lt(1,3) \\ Iw(4,4)Lt(3,4) & 0 & -Iw(4,4)Lt(1,4) \end{bmatrix}$$

$$N_3 = \begin{bmatrix} It(3,3)-It(2,2) & 0 & 0 \\ 0 & It(3,3)-It(1,1) & 0 \\ 0 & 0 & 0 \end{bmatrix}$$

Assuming that (ϕ, θ, ψ) are small in magnitude, the attitude kinematics, expressed by Equation (8), can be linearized around TEA to obtain,

$$\begin{bmatrix} \dot{\phi} \\ \dot{\theta} \\ \dot{\psi} \end{bmatrix} = \begin{bmatrix} 0 \\ 0 \\ -n \end{bmatrix} \phi + \begin{bmatrix} n \\ 0 \\ 0 \end{bmatrix} \psi + \begin{bmatrix} 1 \\ 0 \\ 0 \end{bmatrix} \omega_x + \begin{bmatrix} 0 \\ 1 \\ 0 \end{bmatrix} (\omega_y + n) + \begin{bmatrix} 0 \\ 0 \\ 1 \end{bmatrix} \omega_z \tag{16}$$

Because $\delta\omega_y = \omega_y + n$, we have

$$\begin{aligned} \dot{\phi} &= n\psi + \omega_x \\ \dot{\theta} &= \omega_y + n = \delta\omega_y \\ \dot{\psi} &= -n\phi + \omega_z \end{aligned} \tag{17}$$

Using Equations (15), (17), and (5), a linear differential equation is formed:

$$\frac{d}{dt} \begin{bmatrix} \phi \\ \theta \\ \psi \\ \omega_x \\ \delta\omega_y \\ \omega_z \\ \Omega_1 \\ \Omega_2 \\ \Omega_3 \\ \Omega_4 \end{bmatrix} = A \begin{bmatrix} \phi \\ \theta \\ \psi \\ \omega_x \\ \delta\omega_y \\ \omega_z \\ \Omega_1 \\ \Omega_2 \\ \Omega_3 \\ \Omega_4 \end{bmatrix} + B \begin{bmatrix} \underline{\tau}_w \\ \underline{\tau}_{thruster} \end{bmatrix} + E \ \underline{w} \tag{18}$$

where

$$A = \begin{bmatrix} 0 & 0 & n & 1 & 0 & 0 & \\ 0 & 0 & 0 & 0 & 1 & 0 & 0_{3\times4} \\ -n & 0 & 0 & 0 & 0 & 1 & \\ 3I_g^{-1}n^2N_3 & & & I_g^{-1}nN_1 & & & I_g^{-1}nN_2 \\ -L3I_g^{-1}n^2N_3 & & & -LI_g^{-1}nN_1 & & & -LI_g^{-1}nN_2 \end{bmatrix}$$

$$B = \begin{bmatrix} 0_{3\times4} & 0_{3\times3} \\ -I_g^{-1}L' & I_g^{-1} \\ I_w^{-1} + LI_g^{-1}L' & -LI_g^{-1} \end{bmatrix}$$

$$E = \begin{bmatrix} 0_{3\times3} & 0_{3\times3} & 0_{3\times3} \\ I_g^{-1} & I_g^{-1} & I_g^{-1} \\ -LI_g^{-1} & -LI_g^{-1} & -LI_g^{-1} \end{bmatrix}$$

and N_1, N_2, and N_3 are defined in Equation (15).

Note that roll, pitch, and yaw are coupled even though the products of inertia of the spacecraft are small. This is because more general satellite attitude dynamics model, see Equation (1), with the reaction wheels is used in the derivation.

4. Control Methods

PD Control:

The Proportional Derivative (PD) Control law for the system given by Equation (10) is

$$L'u = -\underline{\omega}\times\left(I_t\underline{\omega} + L'I_w\underline{\Omega}\right) + D\underline{\omega} + K\underline{\phi}_e \quad (19)$$

where $\underline{\omega} = [\omega_x, \omega_y, \omega_z]'$, $\underline{\phi}_e = [\phi, \theta, \psi]'$, $D = d[I_t - L'I_wL]$, and $K = k[I_t - L'I_wL]$.

Then Equation (10) becomes

$$\dot{\underline{\omega}} = -d\underline{\omega} - k\underline{\phi}_e + I_g^{-1}3n^2\underline{c}_3^{\times}I_t\underline{c}_3 + I_g^{-1}\underline{w}. \quad (20)$$

The gravity term, $I_g^{-1}3n^2\underline{c}_3^{\times}I_t\underline{c}_3$, is small compared to the $\underline{\omega}$ or the $\underline{\phi}_e$ terms if we assume small angle change. Also if we assume small external disturbances, we obtain

$$\dot{\underline{\omega}} = -d\underline{\omega} - k\underline{\phi}_e. \quad (21)$$

This is a simple first order system with the dc gain $-\frac{k}{d}$ and the time constant $\frac{1}{d}$. The dc gain establishes the final value the output approaches, and the time constant information concerns the speed of the response. An advantage of a PD controller is in simplicity. It is relatively robust for a single input single output system when the plant is not accurately modeled. This approach is used in the attitude hold mode of our KOMPSAT application.

H_2 Optimal linear quadratic control:

The system state equation is defined by the following equations:

$$\dot{\underline{x}}(t) = A(t)\underline{x}(t) + B(t)\underline{u}(t), \qquad x(0) = x_0 \quad (22)$$

$$z(t) = \begin{bmatrix} C(t)x(t) \\ D(t)u(t) \end{bmatrix} \qquad D'(t)D(t) = I \quad (23)$$

Note that $C'C = Q$ and $D'D = R$ are the weighting matrices. The cost function is given by

$$J_2 = \min_u \left\{ \int_0^T z'(t)z(t)\ dt \right\} \quad (24)$$

The solution is well known for the linear quadratic optimal control problem. The optimal control is given by

$$u^*(t,x) = -B'(t)P(t)\underline{x}(t), \quad (25)$$

where P is given by the following Riccati equation,

$$-\dot{P}(t) = A'(t)P(t) + P(t)A(t) - P(t)B(t)B'(t)P(t) + C'C \quad (26)$$
$$P(T) = 0.$$

H_∞ Optimal control:

The system equation is given by

$$\dot{\underline{x}}(t) = A(t)\underline{x}(t) + B(t)\underline{u}(t) + E(t)\underline{w}(t), \qquad x(0) = x_0 \quad (27)$$

$$z(t) = \begin{bmatrix} C(t)x(t) \\ D(t)u(t) \end{bmatrix} \qquad D'(t)D(t) = I. \quad (28)$$

The cost function is given by

$$J_1 = \int_0^T [\gamma^2 w'(t)w(t) - z'(t)z(t)]\ dt \quad (29)$$

which is an H_∞ criterion [4]. The optimal control is given by the following equations:

$$u^*(t,x) = -B'(t)P_\infty(t)\underline{x}(t), \quad (30)$$

$$w^*(t,x) = -\gamma^{-2}E'(t)P_\infty(t)\underline{x}(t), \quad (31)$$

where the $P_\infty(t)$ is given by the following Riccati equation [4]:

$$-\dot{P}_\infty(t) = A'(t)P_\infty(t) + P_\infty(t)A(t) - P_\infty(t)[B(t)B'(t) - \gamma^{-2}EE']$$
$$P_\infty(t) + C'C, \qquad P_\infty(T) = 0. \quad (32)$$

Mixed H_2/H_∞ Optimal Control:

Mixed H_2/H_∞ control problem is solved using Nash game approach. Two-player, nonzero sum Nash differential games have two performance criteria. The idea of Limebeer *et al.* [4] is to use one performance criterion to reflect H_∞ cost and the other to reflect the H_2 cost.

$$\dot{\underline{x}} = A\underline{x} + B\underline{u} + E\underline{w}, \qquad x(0) = x_0 \quad (33)$$

$$z(t) = \begin{bmatrix} C(t)x(t) \\ D(t)u(t) \end{bmatrix} \qquad D'(t)D(t) = I \quad (34)$$

The first cost function associated with the H_∞ cost is given by

$$J_1 = \int_0^T [\gamma^2 w'(t)w(t) - z'(t)z(t)]\ dt, \quad (35)$$

and the second cost function which is associated with the H_2 cost is given by

$$J_2 = \int_0^T [z'(t)z(t)]\ dt. \quad (36)$$

Then the problem is to find the Nash equilibrium strategies $u^*(t,x)$ and $w^*(t,x)$ in the set of linear memoryless feedback laws, which satisfy the following two inequalities:

$$\begin{aligned} J_1(u^*, w^*) &\le J_1(u^*, w) \\ J_2(u^*, w^*) &\le J_2(u, w^*) \end{aligned}. \quad (37)$$

Then the solution is found to be

$$u^*(t,x) = -B'(t)P_2(t)x(t), \quad (38)$$

$$w^*(t,x) = -\gamma^{-2}E'(t)P_1(t)x(t), \quad (39)$$

where P_1 and P_2 is found from the following coupled Riccati type differential equations [4]:

$$
\begin{aligned}
-\dot{P}_1(t) &= A'(t)P_1(t) + P_1(t)A(t) - P_1(t)\gamma^{-2}EE'P_1(t) \\
&\quad - P_2BB'P_1 - P_1BB'P_2 - P_2BB'P_2 - C'C, \\
-\dot{P}_2(t) &= A'(t)P_2(t) + P_2(t)A(t) - P_1(t)\rho^2\gamma^{-4}EE'P_1(t) \\
&\quad -\gamma^{-2}P_2EE'P_1 - \gamma^{-2}P_1EE'P_2 - P_2BB'P_2 + C'C,
\end{aligned} \tag{40}
$$

with the boundary conditions, $P_1(T) = 0$ and $P_2(T) = 0$.

In mixed H_2/H_∞ optimal control, two cost functions are considered and the optimal controllers are found to minimize these two cost functions. Thus, this optimal control method balances between no additive external disturbance H_2 control and the worst case additive disturbance H_∞ control.

5. Simulation Results

This section contains various numerical simulations for the controllers described in the previous section, The actual parameters of low earth orbiting remote sensing satellite, KOMPSAT, has been used. The KOMPSAT is a sun-synchronous remote sensing satellite with the inclination of 98.13 deg, the altitude of 685km, and the total weight of 509kg. It is scheduled to be launched in August of 1999.

We shall assume that roll, pitch, and yaw angles are available using the conical earth sensor, the fine sun sensor, and the gyros. Furthermore the wheel speeds are also available from the measurement of the reaction wheel tachometer.

On KOMPSAT, a PD controller is used for the attitude hold mode. In this numerical study, we shall show the transient response of the PD controller and compare it with the H_2, H_∞, and mixed H_2/H_∞ controller responses. The simulation parameters are orbital rate, $n = 0.0010636$ rad/s, total moment of inertia for the spacecraft body,

$$
I_t = \begin{bmatrix} 217.30 & 0 & 0 \\ 0 & 95.57 & 0 \\ 0 & 0 & 154.71 \end{bmatrix} \text{ slug ft}^2, \text{ moment of inertia}
$$

matrix for the reaction wheels, $I_w = 0.0077\begin{bmatrix} 1 & 0 & 0 & 0 \\ 0 & 1 & 0 & 0 \\ 0 & 0 & 1 & 0 \\ 0 & 0 & 0 & 1 \end{bmatrix}$ slug ft^2, the parameters for the wheel orientation matrix, L are given as $\alpha = 45^o, \beta = 54.74^o$, and the initial values are chosen as $[0 \quad -n \quad 0 \quad 1 \quad 1 \quad 1]$. In Figure 2, the angular velocities of the spacecraft are plotted with respect to time for a PD controller. Here we let the PD control gain as d=0.1 and k=0.01 in Equation (21). The ω_x has an undershoot and an overshoot before settling down to zero. The response of ω_z closely resemble the response of ω_x. The ω_y has smaller variation then the other angular velocities but it settles down to the orbital rate, $-n$, instead of zero. Figure 3 shows the Euler angle responses, where θ is pitch, ψ is yaw, and ϕ is roll angles. From the initial vaule of 1 degree, ψ and ϕ settle down zero, while θ settles down to $10n$. This result is expected because we know that in steady state, ω_x and ω_z goes to zero and ω_y goes to $-n$ from Figure 2. Thus in steady state $\dot{\underline{\omega}} = 0$ and $\underline{\omega} = [0 \quad -n \quad 0]'$, thus substitute these values into Equation (21), then we obtain $\theta \to \frac{d}{k}n$ in steady state. To make θ approach zero we have to let d<<k, but then we note that the settling time increases. This is because the dc gain is $-\frac{k}{d}$ and the final value approaches zero only when this gain approaches zero. That only happens when either d is equal to zero or when d is equal to infinity. Also when the dc gain approaches zero the time constant, $\frac{1}{d}$, approaches zero, thus the speed of the response increases. Consequently, we note that it is difficult to let the pitch angle approach zero using a PD controller.

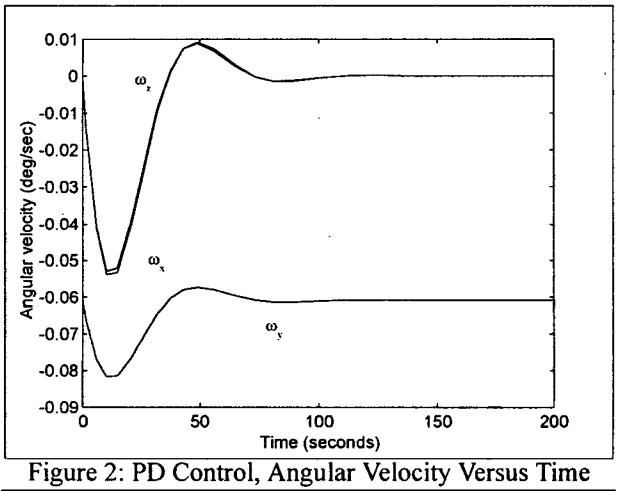

Figure 2: PD Control, Angular Velocity Versus Time

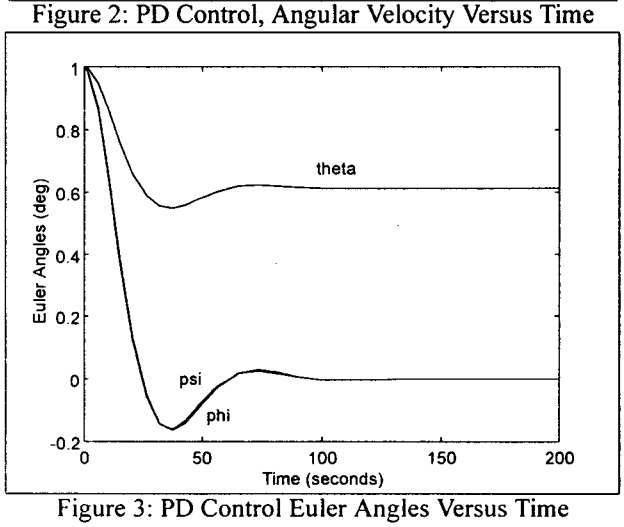

Figure 3: PD Control Euler Angles Versus Time

We use the same simulation parameters as the PD control case. For the comparison purpose, the following Table 1 shows that the angular velocity and time when the angular velocity ω_x is –0.002 deg/sec.

Table 1

Control Method	ω_x (deg/sec)	Time (sec)
H_2 control	-0.002	58.26
H_∞ control	-0.002	82.28
mixed H_2/H_∞ control	-0.002	66.92

Thus H_2 control gives the best performance, H_∞ control gives the worst performance, and mixed H_2/H_∞ control gives the performance in between those two control methods. In PD control, one of the Euler angles, θ, does not approach zero. Thus all three controllers perform better than PD controller. Table 2 shows the times when the roll angle reaches 0.03 degree. Once again the H_2 control gives the fastest time.

Table 2

Control Method	Roll angle (deg)	Time (sec)
H_2	0.03	45.37
H_∞	0.03	99.16
mixed H_2/H_∞	0.03	62.18

We note that the initial action of an H_∞ controller is larger at the start but the overshoot is smaller. Also it settles down to zero faster than the H_2 controller. Once again, the control action of mixed H_2/H_∞ control falls in between the H_2 control and the H_∞ control. Table 3 shows the control action required due to the reaction wheels and the thrusters for the specific times. The times are chosen to match the times of Table 2. Note that H_2 control requires the largest control effort and H_∞ control requires the smallest control effort. Also note that control due to the reaction wheels are zero at those times, implying that the reaction wheels are not being used.

Table 3

control method	Time (sec)	Control due to Reaction Wheels	W_2Control due to thruster		
			x	y	z
H_2	45.4	0.0	.0028	.0006	.0017
H_∞	99.2	0.0	.0001	.0000	.0000
mixed	62.2	0.0	.0012	.0001	.0005

Finally, we show the stability results. Table 4 shows the maximum real part of the closed loop system poles. The PD control has the largest closed loop eigenvalue and H_∞ control has the smallest eigenvalue, but the differences in eigenvalues between H_2 control, H_∞ control, and mixed H_2/H_∞ control are not significant. Thus from the stability point of view all three, H_2 control, H_∞ control, and mixed H_2/H_∞ control, methods give similar stability margins.

Table 4

Control Methods	Maximum real part of the closed loop poles
PD	-0.1
H_2 control	-4.805e-2
H_∞ control	-3.399e-2
mixed H_2/H_∞ control	-6.561e-2

6. Conclusions

This paper presented the beginning of the study of various control methods that can be used in satellite attitude control. The comparison of four different control strategies have been performed. By comparing these performance, we expect to learn more about the differences in various control methods with possibility of applying them in the future KOMPSAT missions. The transient responses of a linear satellite attitude model are studied for four different control methods. We conclude that the PD controller is limited in the sense that it cannot achieve certain angle requirements. An H_2 controller gave the best performance and the H_∞ controller gave the worst performance out of these three control methods, and the mixed H_2/H_∞ controller gave the performance which was in between the H_2 and H_∞ controllers.

7. References

1. Ballois S.L. and G. Duc, "H_∞ Control of an Earth Observation Satellite," *Journal of Guidance, Control, and Dynamics*, Vol. 19, No. 3, May-June 1996, pp. 628—635.
2. Hughes, P. C., Spacecraft Attitude Dynamics, John Wiley & Sons, New York, 1986.
3. Kida, T., I. Yamaguchi , Y. Chida, and T. Sekiguchi, "On-Orbit Robust Control Experiment of Flexible Spacecraft ETS-VI," *Journal of Guidance, Control, and Dynamics*, Vol. 20, No. 5, September-October 1997, pp. 865—872.
4. Limebeer, D.J.N., B.D.O. Anderson, and B. Hendel, "A Nash Game Approach to Mixed H2/H-infinity Control," *IEEE Transactions on Automatic Control*, Vol. 39, No. 1, January 1994, pp. 69—82.
5. Wie B., K. W. Byun, V. W. Warren, D. Geller, D. Long, and J. Sunkel, "New Approach to Attitude/Momentum Control for the Space Station," *Journal of Guidance, Control, and Dynamics*, Vol. 12, No. 5, September-October 1989, pp. 714—722.